Electronic Journal of Biotechnology 63 (2023) 30–40

Contents lists available at ScienceDirect

Electronic Journal of Biotechnology

journal homepage: www.elsevier.com/locate/ejbt

Research Article

NIFK, an independent prognostic biomarker of hepatocellular carcinoma, is correlated with immune infiltration

Fei Cheng [1], Lebin Yuan [1], Zhao Wu, Huizi Li, Wei Shen *

Department of General Surgery, The Second Affiliated Hospital of Nanchang University, Nanchang, Jiangxi 330006, China

GRAPHICAL ABSTRACT

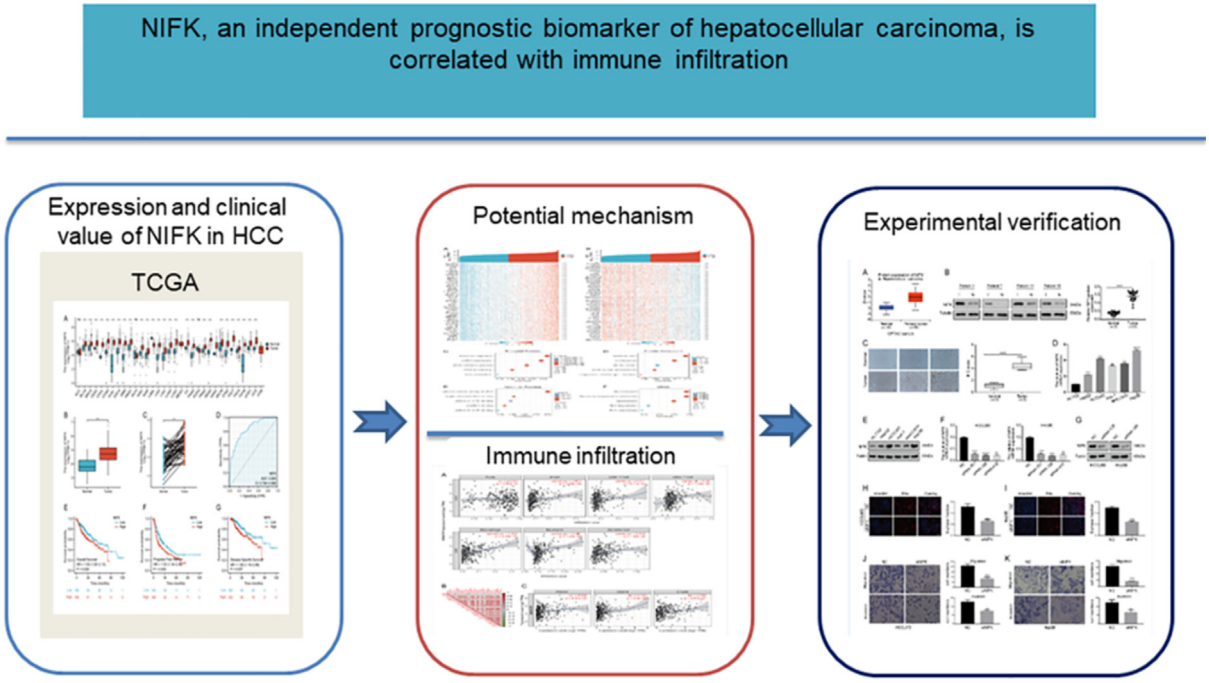

ARTICLE INFO

Article history:
Received 16 September 2022
Accepted 23 January 2023
Available online 14 April 2023

Keywords:
Biomarker
Cancer

ABSTRACT

Background: The molecular mechanisms that lead to hepatocellular carcinoma (HCC), a highly common malignant tumor, are currently unclear. In fact, while the nucleolar protein that interacts with the FHA domain of pKi-67 (NIFK) is known to promote lung cancer progression, its specific role in HCC remains unknown.

Results: In HCC tissues, NIFK was significantly overexpressed in comparison with normal tissues. In The Cancer Genome Atlas (TCGA) database, NIFK expression showed a good prediction value according to an ROC curve and it was linked to poor progression-free interval, disease-specific survival and overall

Peer review under responsibility of Pontificia Universidad Católica de Valparaíso.

* Corresponding author.
E-mail address: ndefy95006@ncu.edu.cn (W. Shen).
[1] These authors contributed equally to this work.

https://doi.org/10.1016/j.ejbt.2023.01.003

HCC
Hepatocellular carcinoma
Immune infiltration
Liver cancer
Malignant
NIFK
Prognosis
Risk factors
Tumor

survival. Furthermore, the level of NIFK expression in HCC was significantly correlated with tumor stage, AFP (ng/mL), OS event, DSS event and PFI event. Based on GSEA evaluations, differentially expressed NIFK genes exhibited enrichment for fatty acid metabolism, oxidative phosphorylation as well as cancer, cell cycle, MAPK, TGF, WNT and NOTCH signaling pathways. The TIMER database analysis further revealed positive associations between NIFK expression and the immune cells, such as dendritic cells, neutrophils, macrophages, CD4+ T cells, CD8+ T cells and B cells. Also, the NIFK expression was positively correlated with immune checkpoints (PD1/PD-L1 and CTLA4). The experimental verification determined that NIFK knockdown could thwart HCC cellular properties of proliferation, metastasis and invasiveness. Univariate and multivariate Cox hazard regression validated NIFK expression as an independent prognostic marker in HCC.

Conclusions: NIFK has theragnostic potential as a separate prognostic factor or novel biomarker involved in the immune infiltration of HCC.

How to cite: Cheng F, Yuan L, Wu Z, et al. NIFK, an independent prognostic biomarker of hepatocellular carcinoma, is correlated with immune infiltration. Electron J Biotechnol 2023;63. https://doi.org/10.1016/j.ejbt.2023.01.003.

1. Introduction

Liver cancer, a highly common malignant tumor, currently ranks fourth in terms of cancer-related death, and its most frequently encountered subtype is hepatocellular carcinoma (HCC), whose morbidity and mortality seriously affect people's health, especially in Africa and East Asia [1,2,3,4,5]. Many risk factors, including viral hepatitis infection, nonalcoholic steatohepatitis, and alcohol addiction, are considered important contributors to the development of HCC [6,7]. Despite remarkable HCC theragnostic efforts, the five-year survival rates have remained unfavorable over the past few years, mainly as a result of high rates of metastasis and recurrence [8]. At present, the molecular mechanisms behind HCC initiation and progression remain largely unclear; hence, it is essential to explore these mechanisms to identify novel prognostic biomarkers and therapeutic targets to develop new forms of treatment.

Ki67, a commonly used marker of cell proliferation, plays a pivotal role in cancer; two-hybrid screening is used to identify the nucleolar protein interacting with the FHA domain of pKi-67 (NIFK), wherein the FHA domain of Ki67 is used as a substrate [9,10,11]. The binding of NIFK to this domain occurs through glycogen synthase kinase GSK-3 and cyclin-dependent kinase 1, which are two key regulators of mitosis for Ki-67, and the sequential phosphorylation of Thr238 and Thr234 of NIFK is also necessary for Ki-67 recognition [12]. NIFK is transcriptionally upregulated through c-Myc and estrogen, suggesting that it may affect cell proliferation [13,14]. In addition, through interplay with nucleophosmin 1 (NPM1/B23), a versatile-functioning protein with endoribonuclease properties, NIFK can also maintain proliferation/pluripotency for embryonic stem cells [15,16]. Moreover, during metastasis and Ki-67-dependent cellular proliferation, NIFK acts through CK1α/β-catenin to promote lung cancer progression [17]. However, its potential prognostic value and biomolecular mechanisms in HCC remain unrevealed.

Within the current study, LIHC datasets were extracted via The Cancer Genome Atlas (TCGA) before being analyzed with an R software package. Combined with data from an online database, correlations between NIFK expression, clinical characteristics and prognosis were examined in cases of HCC. The NIFK coexpressed genes in the HCC cases were also analyzed to assess their signal transduction pathways as well as biological functions. Furthermore, we investigated the immune infiltrates and immune checkpoint expression levels of NIFK in HCC. Finally, experimental verification confirmed that NIFK was implicated in HCC cellular properties of proliferation, metastasis and invasiveness. Therefore, NIFK may act as a promising biomarker and therapeutic targets for HCC.

2. Materials and methods

2.1. Human tissue specimens

We obtained 20 pairs of HCC tissues from patients undergoing resection surgery at the Second Affiliated Hospital of Nanchang University between March 2022 and August 2022. Informed consents were signed by all patients, and the study protocol was approved by the Ethics Committee of the Second Affiliated Hospital of Nanchang University.

2.2. Expression and prognostic value of NIFK in HCC

The TCGA database (https://portal.gdc.cancer.gov/) was employed to acquire transcriptome data of LIHC and its corresponding clinical information [18]. We used an R package to analyze NIFK dysregulations across tumors and healthy tissues. Furthermore, the TCGA LIHC dataset was analyzed to explore NIFK expression in paired and unpaired HCC and normal tissues. An ROC curve and Cox modeling were then employed to evaluate the diagnostic and prognostic values for NIFK within LIHC. The correlations between NIFK expression and clinicopathological characteristics were examined using clinical data of LIHC datasets from the TCGA.

2.3. Functional enrichment analysis of coexpressed NIFK genes

The TCGA LIHC dataset was analyzed using an R package to investigate coexpressed genes associated with NIFK expression. In this case, statistical correlations were tested with Pearson's correlation coefficient before drawing volcano and heatmaps through the ggplot2 package of R software. The Gene Ontology (GO) function and Kyoto Encyclopedia of Genes and Genomes (KEGG) pathway enrichment evaluations for coexpressed genes were then performed by the cluster Profiler R package (version: 3.6.3) [19]. In R software, the results were visualized using ggplot2. We used the UALCAN database (http://ualcan.path.uab.edu) [20,21] to assess the prognostic value of NIFK coexpressed genes with strong correlations.

2.4. Enrichment analysis of gene sets and infiltration of immune cells

The potential functions of NIFK were explored by dividing the TCGA LIHC data into a high-expression group or a low-expression

group based on NIFK expression profiles to identify differentially expressed genes. GSEA (www.gsea-msigdb.org/gsea/index.jsp) [14] was conducted to probe whether these genes were enriched in important pathways. The associations between NIFK expression and immune infiltration were then analyzed for HCC cases through the TIMER online database (https://cistrome.shinyapps.io/timer/) [22]. Furthermore, the links between NIFK expression and the expression levels of immune checkpoint genes (such as PDCD1, CD274, and CTLA4) were assessed.

2.5. Cell culture and transfection

The human HCC cell lines (HepG2, Huh-7, Hep3B, HCCLM3, MHCC97H) and normal liver cell (HL7702) were obtained through the Shanghai Institute of Cell Biology, China. Cell cultures were established in DMEM (Gibco) and augmented through 10% FBS (Gibco), together with 100 units/mL penicillin and streptomycin, prior to incubation at 37°C and under 5% CO_2. Short interfering RNAs (siRNAs) targeting NIFK along with negative control siRNA-NC were obtained from GenePharma (Shanghai) and used for the transfection of HCC cells in the presence of Lipofectamine 3000 (Invitrogen) according to the manufacturer's guidelines. The NIFK siRNA sequences are in Table 1.

2.6. RNA extraction and real-time PCR

The total RNA was extracted from tissue samples using the TRIzol® reagent (Thermo Fisher Scientific) according to the manufacturer's specifications. This was followed by reverse transcription using the Prime Script RT kit (Takara™), with the resulting cDNA treated with gDNA prior to amplification on an ABIPRISM 7500 autofluorescence PCR device. In this case, PCR was executed with a SYBR Premix Ex Taq™ kit (Takara™) using the following primers: NIFK: GGGCCAATCCTGTCGCTTAAT (forward) and GTTATGCGCTTGCGAACCT (reverse); GDPAH: GGAGCGAGATCCCTCCAAAAT (forward) and GGCTGTTGTCATACTTCTCATGG (reverse). The 2-ΔΔCT methodology was employed for relative quantification of mRNA expression profiles.

2.7. Protein extraction and western blotting

Five kinds of HCC cells, normal liver cell and 20 pairs of samples were lysed using lysis buffer (Beyotime™, Shanghai, China). Total protein concentration was obtained by BCA method. This was followed by protein separation (30 μg) via 10% SDS-PAGE and subsequent transfer onto PVDF membranes. Using 5% skimmed milk, blocking of the membranes was then carried out at 37°C for 60 min prior to overnight incubation at 4°C with primary antibodies (NIFK, 1:1,000; Tubulin, 1:2,000; Proteintech). After washing the membranes, incubation was performed with the secondary antibody, and protein bands were eventually detected through chemiluminescence.

2.8. Transwell assays

The migration assay was performed by adding a cell suspension (5×10^4) prepared in serum-free medium into the upper chamber. For the invasion assays, Matrigel was diluted 1:8 to coat the membrane in the upper transwell chamber prior to air-drying for 3 h. This was followed by the addition of 5×10^5 cells (200 μL suspension) to the upper chamber, and after a 24-h (for migration) or 48-h (for invasion) incubation, the chamber was removed and rinsed twice with PBS. The cells within the upper layer of the microporous membrane of the chamber were carefully wiped with a cotton swab and used for cell fixation. This was performed in a 24-well plate for 20 min using 4% paraformaldehyde (or 95% alcohol) before a 30-min staining with crystal violet solution. Photographs were taken using an inverted microscope, three fields of view were randomly counted per sample, and the mean values were used for statistical analyses.

Table 1
The NIFK siRNA sequences are as follows.

Gene name	Sequences	
	sense (5'-3')	antisense (5'-3')
NIFK -415	GCAGCCAUCAUAUCCAUCATT	UGAUGGAUAUGAUGGCUGCTT
NIFK -701	CCAGUUUGUACACCAACAUTT	AUGUUGGUGUACAAACUGGTT
NIFK -126	CUCCUGGAGUAGUCUAUGUTT	ACAUAGACUACUCCAGGAGTT
NIFK-NC	UUCUCCGAACGUGUCACGUTT	ACGUGACACGUUCGGAGAATT

2.9. EdU assay

After culturing 5,000 cells in 96-well plates (100 μL/well) at 37°C and under 5% CO_2, cell treatment was performed with EdU reagent (Ribobio) according to the specifications of the manufacturer. The cells were photographed in wells using fluorescence microscopy.

2.10. Immunohistochemistry (IHC) staining

IHC staining was performed using the standard avidin-biotin complex method. Concentration of antibody incubation is 1:100 (anti-NIFK, Proteintech). The staining intensity and percentage of positive cells were scored as previously described [23].

2.11. Statistical analyses

The datasets were evaluated using SPSS® 22.0 software (SPSS Inc.™, Chicago, IL, USA) and GraphPad Prism 7® (GraphPad Software™, San Diego, CA, USA). The results are presented as the means ± standard deviations. Variations across the groups were analyzed at 5% significance levels using the chi-square test or ANOVA. Each experiment was executed three times.

3. Results

3.1. Expression levels of NIFK in HCC

TCGA datasets were first used to analyze NIFK expression in human tumors, and compared to corresponding normal tissues, NIFK was significantly increased in most cancers, including liver, colorectal, lung, head and neck, breast, gastric, pancreatic, central nervous system, and cervical cancer and other tumors (Fig. 1A). Considering that in China, HCC morbidity and mortality are high, we further examined HCC cases. TCGA data confirmed that NIFK expression was markedly upregulated within unpaired (Fig. 1B) and paired (Fig. 1C) HCC and normal samples. These results indicated that HCC progression could be linked to NIFK expression. Therefore, the prognostic and diagnostic values of NIFK were assessed based on ROC curves as well as Cox regression models. The results of the ROC curves indicated that NIFK had good predictive value in HCC, with an area under the curve of 0.840 (95% CI: 0.784–0.896) (Fig. 1D). Similarly, analyses based on Cox regression models suggested that high levels of NIFK expression were linked to worse survival results, including poorer overall survival (OS; HR = 1.50 (1.05–2.13); P = 0.026), disease-specific survival (DSS; HR = 1.89 (1.19–2.99), P = 0.007), and progression-free intervals (PFS; HR = 1.53 (1.14–2.06), P = 0.005) (Fig. 1E-G).

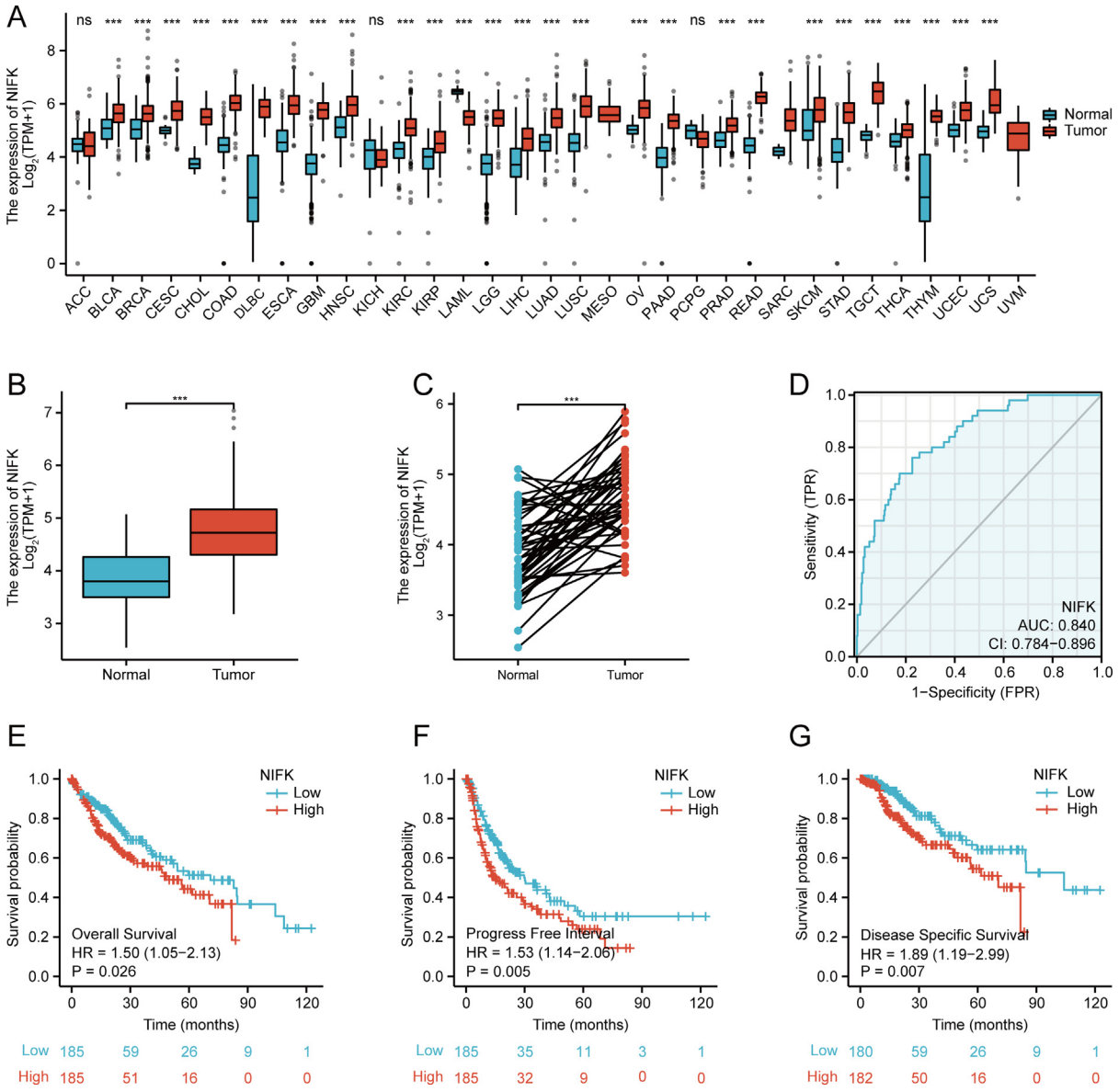

Fig. 1. NIFK expression and survival in HCC cases. (A) The TCGA datasets were used to analyze NIFK expression in various cancers; (B, C) HCC tissues and corresponding normal tissues, including unpaired (B) and paired (C) samples, were compared in terms of NIFK expression; (D) ROC curve analysis of NIFK in HCC; (E) OS analysis for NIFK; (F) DSS analysis for NIFK; (G) PFI analysis for NIFK. *P < 0.05; **P < 0.01; ***P < 0.001; ****P < 0.0001; ns, not significant.

3.2. Correlations of NIFK expression with clinical outcomes

The correlations between NIFK expression and clinical characteristics were also investigated by analyzing clinical data from TCGA HCC samples. The clinical characteristics included age, sex, T, N and M stages, vascular invasion, AFP (ng/mL), histological grade, pathological stage, OS, DSS, and PFI events. Fig. 2A and Fig. 2B indicated that NIFK expression had no correlation with the age and gender of HCC patients. However, Fig. 2D showed that NIFK expression in the N0 and N1 groups was significantly higher than that in the normal groups. Also, Fig. 2E displayed that NIFK expression in the M0 and M1 groups was higher than that in the normal groups. Moreover, the results showed significantly higher NIFK expression in the T3 and T4 groups than in the T1 and T2 groups (Fig. 2C) as well as in the stage III and IV groups than in the stage I and II groups (Fig. 2F). Similarly, the G3 and G4 groups had higher NIFK expression than the G1 and G2 groups (Fig. 2G). In addition, NIFK expression in the group with vascular invasion was significantly higher than that in the group without vascular invasion (Fig. 2H). NIFK expression in AFP > 400 group was significantly higher than that in AFP < 400 group (Fig. 2I). In the OS, DSS and PFI event, whether is it in the alive group or in the dead group, NIFK expression was significantly higher than that in the normal group (Fig. 2J-L). However, NIFK expression in the dead group was significantly higher than that in the alive group during OS event (Fig. 2J). Furthermore, we analyzed the clinical and gene expression profiles for HCC in TCGA before assigning patients to a high-expression or low-expression group based on the median value of NIFK expression. In this case, the Wilcoxon signed-rank test and logistic regression determined how NIFK expression was linked to clinical characteristics (Table 2). Univariate Cox hazard regression analysis showed that the M stage (M1), T stage (T3 and T4) and pathologic stages (stages III and IV) as well as higher NIFK expression were significantly correlated with poor OS in HCC patients. Moreover,

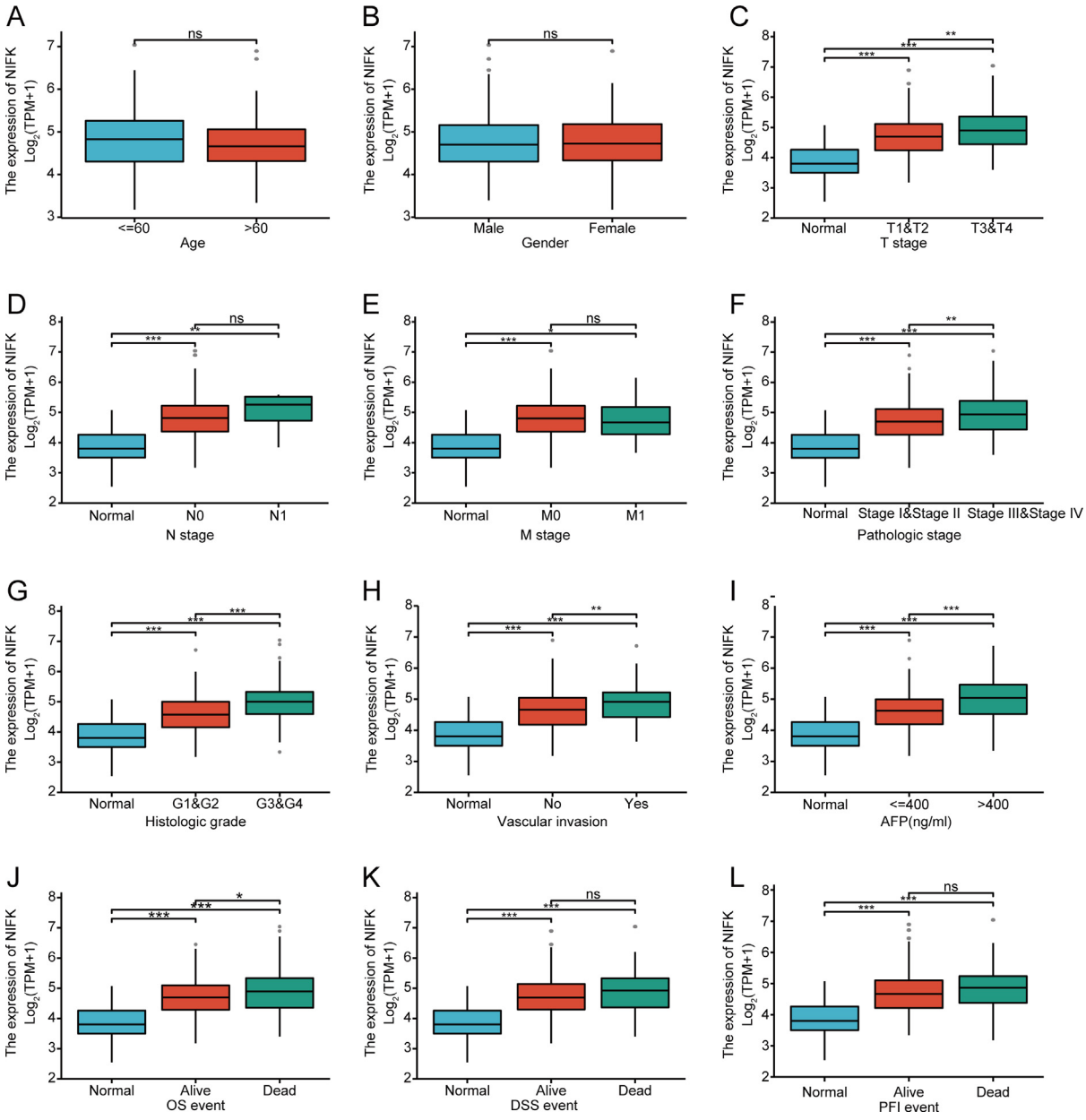

Fig. 2. Relationship between NIFK expression and clinicopathological characteristics of HCC. The relationship between NIFK expression and clinical characteristics (A) age; (B) gender; (C) T stage; (D) N stage; (E) M stage; (F) pathologic stage; (G) histologic grade; (H) vascular invasion; (I) AFP (ng/mL); (J) OS event; (K) DSS event; (L) PFI event were analyzed with R; *$P < 0.05$; **$P < 0.01$; ***$P < 0.001$; ****$P < 0.0001$; ns, not significant.

multivariate Cox analysis indicated that the M stage (M1), T stage (T3 and T4), pathologic stages (stages III and IV) and higher NIFK expression were also associated with poor OS. Overall, NIFK expression was shown to be an independent prognostic factor for HCC patients (HR = 1.956, 95% CI = 1.242–3.081, $P = 0.004$) (Table 3).

3.3. Enrichment of NIFK-related coexpressed genes

By analyzing the HCC datasets in the TCGA using R software, we identified coexpressed genes associated with NIFK expression, and protein-coding genes were included in the study. There were 8,022 genes that satisfied the |cor| > 0.3 and $P < 0.05$ criteria. Using this threshold, 7,652 and 370 genes were positively and negatively correlated with NIFK expression, respectively. After adjusting the threshold to |cor| > 0.8 and $P < 0.05$, only three genes, namely, NOP58 (cor = 0.829, $P < 0.05$), SSB (cor = 0.811, $P < 0.05$) and WDR75 (cor = 0.815, $P < 0.05$), showed a significant correlation and volcano plot revealed the three genes strongly correlated with NIFK expression (Fig. 3G). The link between these three genes and survival in HCC was further evaluated by using the UALCAN database, and these three genes were significantly correlated with poor OS (Fig. 3H-J). A heatmap map was then produced to show the top-ranking 50 genes for which a positive or negative association with NIFK expression was observed (Fig. 3A-B).

The molecular mechanism through which NIFK exerts its effects was explored by analyzing the top 200 coexpressed genes that were positively correlated with NIFK expression. The GO function analysis showed that coexpressed genes were primarily enriched in single-stranded RNA binding, ribosome biogenesis, ncRNA pro-

Table 2
Correlation between NIFK expression and clinicopathologic characteristics of patients with HCC.

Characteristic	Low expression of NIFK	High expression of NIFK	*P* value
n	187	187	
T stage, n (%)			0.061
T1	103 (27.8%)	80 (21.6%)	
T2	41 (11.1%)	54 (14.6%)	
T3	36 (9.7%)	44 (11.9%)	
T4	4 (1.1%)	9 (2.4%)	
N stage, n (%)			0.625
N0	120 (46.5%)	134 (51.9%)	
N1	1 (0.4%)	3 (1.2%)	
M stage, n (%)			1.000
M0	127 (46.7%)	141 (51.8%)	
M1	2 (0.7%)	2 (0.7%)	
Pathologic stage, n (%)			0.125
Stage I	96 (27.4%)	77 (22%)	
Stage II	38 (10.9%)	49 (14%)	
Stage III	36 (10.3%)	49 (14%)	
Stage IV	3 (0.9%)	2 (0.6%)	
Gender, n (%)			1.000
Female	60 (16%)	61 (16.3%)	
Male	127 (34%)	126 (33.7%)	
Age, n (%)			0.133
≤ 60	81 (21.7%)	96 (25.7%)	
>60	106 (28.4%)	90 (24.1%)	
BMI, n (%)			0.168
≤25	83 (24.6%)	94 (27.9%)	
>25	88 (26.1%)	72 (21.4%)	
AFP (ng/ml), n (%)			0.003
≤400	123 (43.9%)	92 (32.9%)	
>400	23 (8.2%)	42 (15%)	
Vascular invasion, n (%)			0.052
No	116 (36.5%)	92 (28.9%)	
Yes	48 (15.1%)	62 (19.5%)	
Age, median (IQR)	64 (53, 69)	60 (51, 68)	0.097

cessing, acting on RNA, nucleolar parts, preribosome and catalytic activity (Fig. 3C-E). Similarly, the KEGG analysis showed that RNA transport, ribosome biogenesis in eukaryotes, spliceosome, RNA degradation and RNA polymerase were the main enriched pathways (Fig. 3F).

3.4. Enrichment analysis of NIFK signaling pathways

To investigate the potential signaling pathways of the NPM1 gene, GSEA of the differentially expressed genes was performed, showing that NIFK differentially expressed genes were enriched in fatty acid metabolism, oxidative phosphorylation, cancer, and the cell cycle as well as in the WNT, MAPK, TGF and NOTCH signaling pathways. Collectively, these findings broaden the knowledge base of the potential biomolecular mechanisms for NIFK in HCC (Fig. 4).

3.5. Immune cell infiltration analysis

The infiltration of immune cells is associated with HCC progression [24,25]; thus, we explored how NIFK expression was related to immune cell infiltration. The results from the TIMER database indicated a positive correlation between NIFK expression and dendritic cells (r = 0.318, *P* = 1.92E-09), neutrophils (r = 0.801, *P* = 1.24E-08), macrophages (r = 0.323, *P* = 9.90E-10), B cells (r = 0.312, *P* = 3.29E-09), CD4+ T cells (r = 0.260, *P* = 1.03E-06) and CD8 + T cells (r = 0.211, *P* = 8.71E-05) (Fig. 5A). Moreover, we explored the association between NIFK and immune checkpoints in HCC cases. A heatmap of NIFK expression and immune checkpoints is shown in Fig. 5B. CTLA4 and PD1/PD-L1 are key immune checkpoints involved in immune escape, and we used the TIMER database to evaluate their relationship with NIFK expression. The results showed robust positive associations among NIFK expression, PD1/PD-L1 and CTLA4 (Fig. 5C).

3.6. Effects of knocking down NIFK

To investigate whether NIFK affects HCC cellular properties of proliferation, metastasis and invasiveness, we firstly analyzed the protein expression of NIFK in HCC tissues and normal tissues in Ualcan database (Fig. 6A). Meanwhile, we obtained 20 pairs of HCC tissues and corresponding normal tissues, NIFK protein levels were detected by western blot and IHC (Fig. 6B-C). The results showed that the expression of NIFK was significantly upregulated in HCC. Then, its expression in normal and cancerous cells was

Table 3
Associations with clinicopathologic characteristics in HCC patients using univariate and multivariate Cox regression.

Characteristics	Total(N)	Univariate analysis		Multivariate analysis	
		Hazard ratio (95% CI)	*P* value	Hazard ratio (95% CI)	*P* value
Age	373				
≤60	177	Reference			
>60	196	1.205 (0.850-1.708)	0.295		
Gender	373				
Female	121	Reference			
Male	252	0.793 (0.557-1.130)	0.200		
Pathologic stage	349				
Stage I & Stage II	259	Reference			
Stage III & Stage IV	90	2.504 (1.727-3.631)	**<0.001***	1.374 (0.187-10.073)	0.755
T stage	370				
T1&T2	277	Reference			
T3&T4	93	2.598 (1.826-3.697)	**<0.001***	2.177 (0.294-16.112)	0.446
M stage	272				
M0	268	Reference			
M1	4	4.077 (1.281-12.973)	**0.017***	1.936 (0.593-6.320)	0.274
N stage	258				
N0	254	Reference			
N1	4	2.029 (0.497-8.281)	0.324		
NIFK	373				
Low	187	Reference			
High	186	1.509 (1.059-2.149)	**0.023***	1.956 (1.242-3.081)	**0.004***

* *P* < 0.05 has statistical significance.

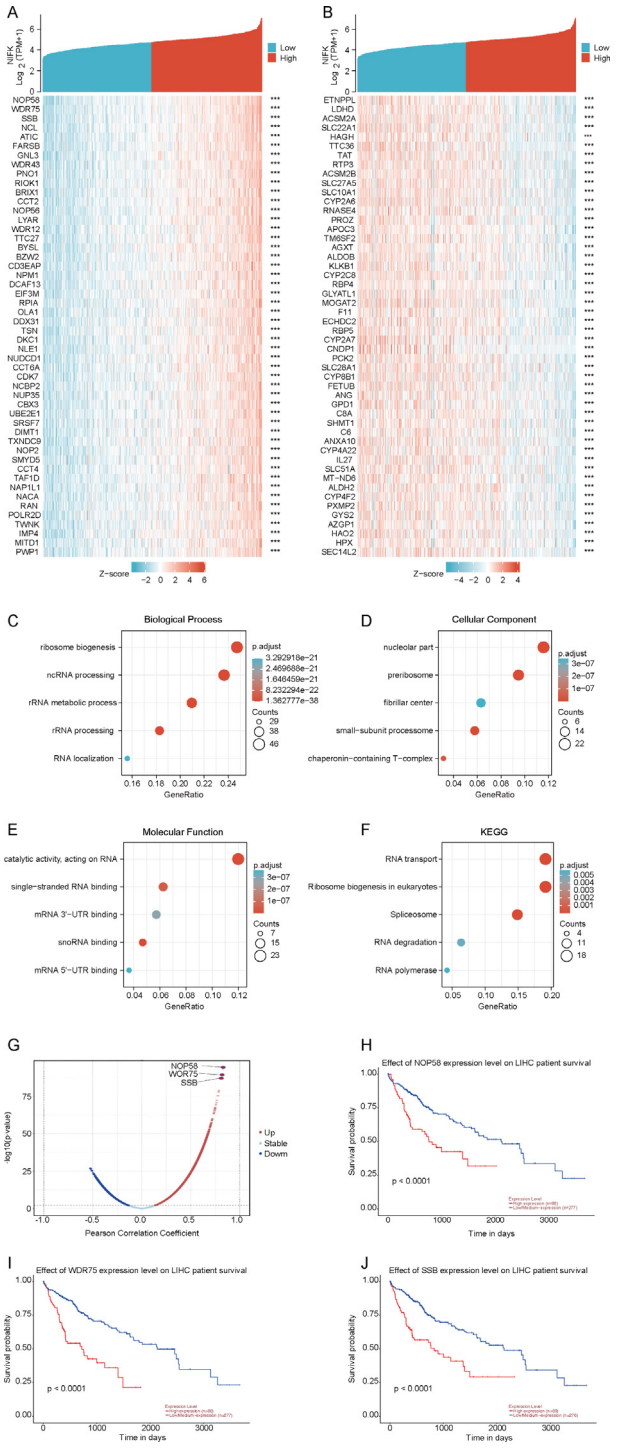

Fig. 3. Enrichment of NIFK coexpression genes in HCC. (A-B) Heatmap map showing the top 50 genes for which positive and negative correlations with NIFK expression were observed in TCGA datasets; (C-F) GO/KEGG enrichment analyses of NIFK coexpressed genes; (G) Volcano plot showing NIFK expression associated with NIFK coexpressed genes in TCGA data; (H-J); The ULCAN database was used to evaluate survival and the genes most strongly correlated with NIFK expression, i.e., NOP58 (H) WDR75 (I), and SSB (J).

compared by western blotting and qPCR (Fig. 6D-E). The results demonstrated that NIFK mRNA and protein levels were significantly upregulated in HCC cells in comparison to normal liver cell. HCCLM3 and Hep3B cells were used for the subsequent cell function experiments. The expression of NIFK in HCCLM3 and Hep3B cells was knocked down by siRNA transfection technology and the gene silencing efficiency was detected by Western blotting and qPCR (Fig. 6F-G). Furthermore, the capacity of cellular HCC to proliferate, invade and metastasize after the knockdown of NIFK in HCCLM3 and Hep3B cells was assessed by using EdU and transwell assays. For the first assay, the cell proliferation rate in HCCLM3 and Hep3B cells in the siNIFK group was shown to be lower compared with the control group (Fig. 6H-I). The transwell assays further revealed a significantly weaker process of cell migration and invasion for HCCLM3 and Hep3B cells compared with those in the NC group (Fig. 6J-K).

4. Discussion

Although HCC is a common malignant tumor, its prognosis is still not satisfactory due to its complex underlying molecular mechanism. Currently, there are various options to treat HCC, including chemotherapy and immunotherapy; however, the outcomes for patients with HCC are still generally poor due to high recurrence and metastasis rates after treatment [5,26,27]. More than 200 genes have been associated with HCC progression; however, the molecular mechanisms implicated in HCC are diverse, and its specific pathways and prognosis-related molecules are still unclear [28]. Therefore, exploring the molecular mechanism of HCC remains important, especially for identifying novel biomarkers that may provide effective diagnostic and therapeutic targets for HCC.

NIFK is also referred to as MKI67IP and Nopp34, and it is a novel nucleolar protein that can interact with the forkhead-associated domain of the Ki-67 antigen [9]. Previous studies have shown that nucleolar proteins can promote the progression of lung cancer during metastasis and proliferation [17], suggesting that NIFK may be a novel oncogene. However, the potential mechanism through which NIFK contributes to HCC occurrence and development is poorly understood. This study investigated the expression of NIFK in pan-cancer data using bioinformatics, as NIFK is highly expressed in various human tumors. By focusing on the expression of NIFK, the results indicated a significantly higher level of expression in HCC compared with corresponding normal tissues. The ROC curve analysis and survival curves showed that NIFK may act as a promising diagnostic and prognostic biomarker.

An enhanced knowledge base concerning biomolecular mechanistics for NIFK during HCC came from an analysis of NIFK coexpressed genes in TCGA HCC datasets. We used a volcano plot to display coexpressed genes of NIFK. NOP58, WDR75, and SSB were most strongly associated with NIFK genes and were related to poor prognosis in HCC. NOP58 ribonucleoprotein is a protein-coding gene located on chromosome 2 [29]. Wang et al. [30] found that overexpression of NOP58 acted as a prognostic biomarker in HCC, whereas the functions of WDR75 and SSB in HCC have not been reported. A GSEA pathway enrichment analysis demonstrated that the differentially expressed genes of NIFK were predominantly enriched within fatty acid metabolism, oxidative phosphorylation, cancer, and the cell cycle as well as in the WNT, MAPK, TGF and NOTCH signaling pathways. Previous studies have shown that the WNT signaling pathway is important for HCC progression [31]. The MAPK, TGF, and NOTCH signaling pathways are also associated with the molecular mechanism of HCC [32,33,34]. The immune microenvironment is also important for HCC progression [35,36]. In this study, analysis of the TIMER database revealed positive correlations between NIFK expression and dendritic cells, neutrophils, macrophages, B cells, CD4+ T cells and CD8+ T cells. Such results

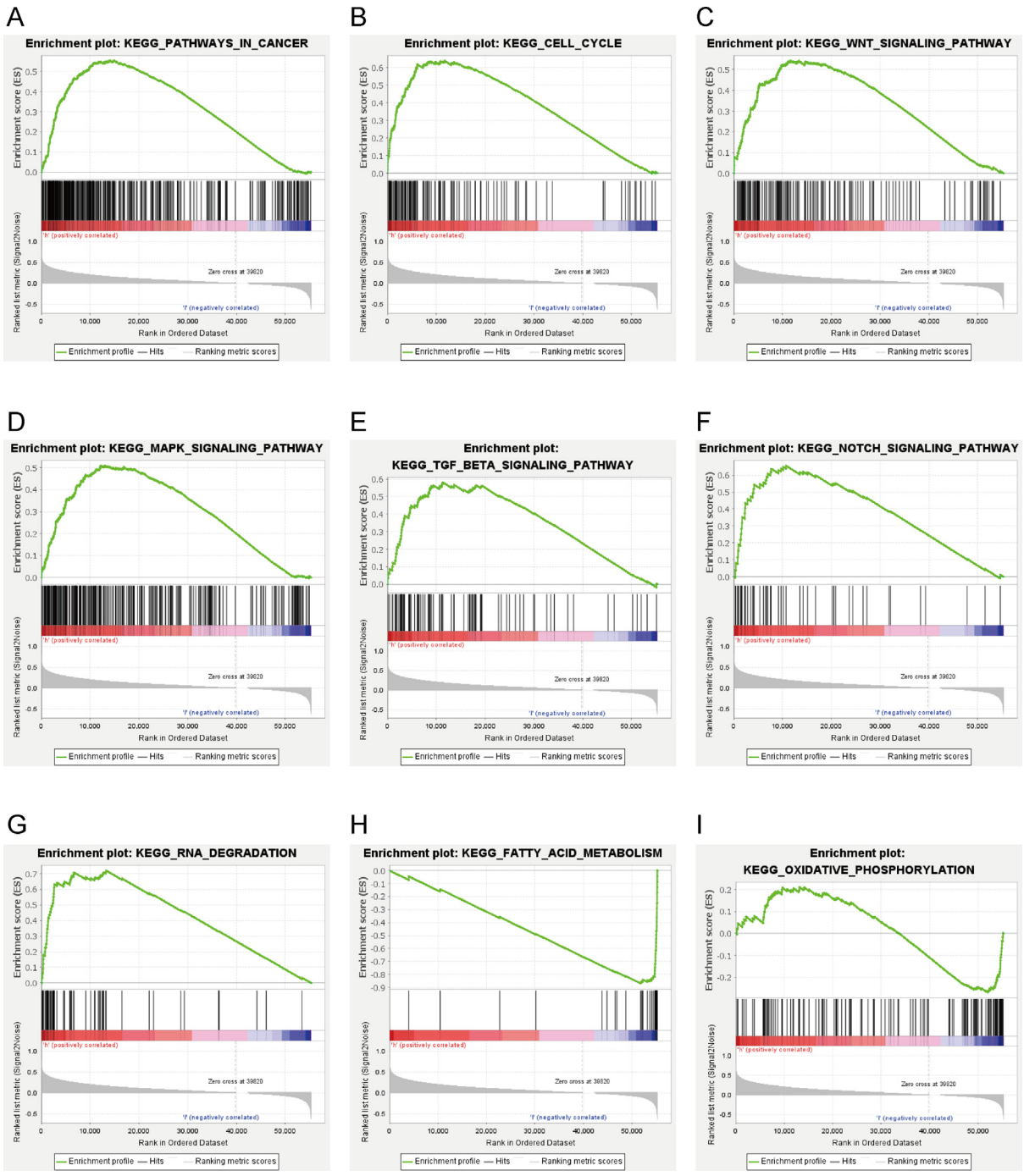

Fig. 4. Gene set enrichment analysis of differential genes of NIFK. (A) Pathway in cancer; (B) Cell cycle; (C) WNT signaling; (D) MAPK signaling; (E) TGF signaling; (F) NOTCH signaling pathways; (G) RNA degradation; (H) Fat acid metabolism; (I) Oxidative phosphorylation.

indicate that NIFK may be implicated in the immune response of the HCC tumor microenvironment, especially macrophages and CD4+ T, CD8+ T and B cells. Immune checkpoint inhibitors are a hot spot in the treatment of HCC [36]. In this case, the TIMER database analyses also showed positive correlations between NIFK expression, PD1/PD-L1 and CTLA4. These results suggest that NIFK could be part of the immune escape mechanisms during HCC progression.

In the TCGA HCC datasets, we found that NIFK expression in the group without vascular invasion was markedly downregulated in comparison to the vascular invasion cohort, which indicated that the expression of NIFK may gradually increase with HCC progres-

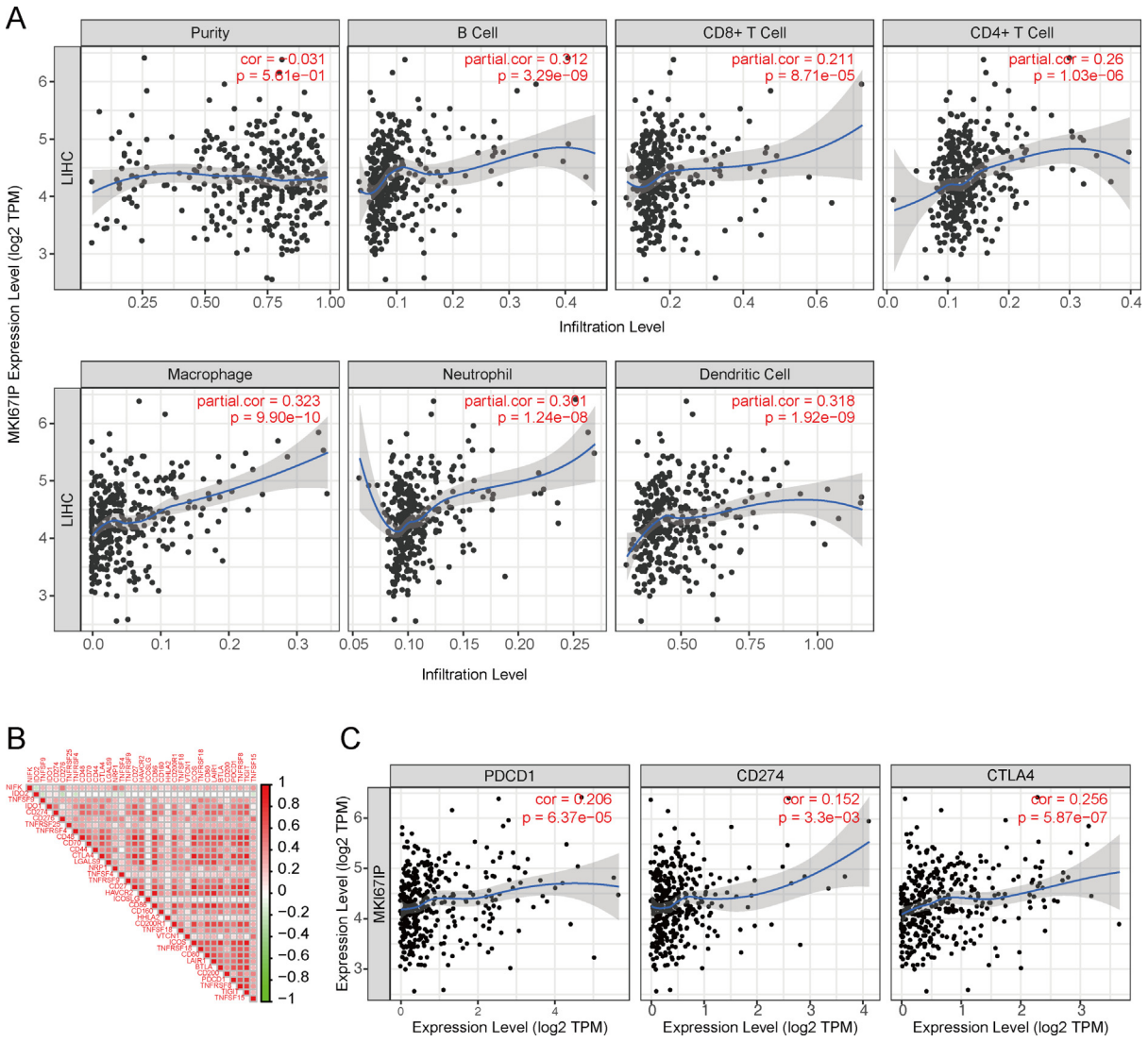

Fig. 5. Relationship between NIFK expression and infiltration of immune cells. (A) To determine how NIFK expression was linked to immune infiltrating cells, the TIMER database was used. (B) Heatmap of NIFK and immune checkpoints. (C) Correlation of NIFK and PDCD1, CD274 and CTLA4.

sion. Therefore, we used experimental verification to confirm that NIFK has functions in HCC proliferation, invasion, and metastasis. Protein expression of NIFK in HCC was evaluated and detected by Ualcan database, western blotting and IHC. The levels of NIFK expression in various HCC cells were first examined using western blotting and qRT-PCR. NIFK was upregulated in various HCC cells. EdU and Transwell assays provided evidence that knocking down NIFK expression could inhibit HCC proliferation, invasion, and metastasis.

In conclusion, our results showed that NIFK was highly expressed in HCC and linked to tumor stage and poor prognosis. An additional analysis suggested that NIFK was likely to act as a separate prognostic factor within HCC. Furthermore, the knockdown of NIFK expression inhibited HCC cell proliferation, invasion, and metastasis. Our results indicate that NIFK is a promising biomarker of theragnostic value. However, the specific mechanisms underlying NIFK in HCC should be further verified through experimental studies.

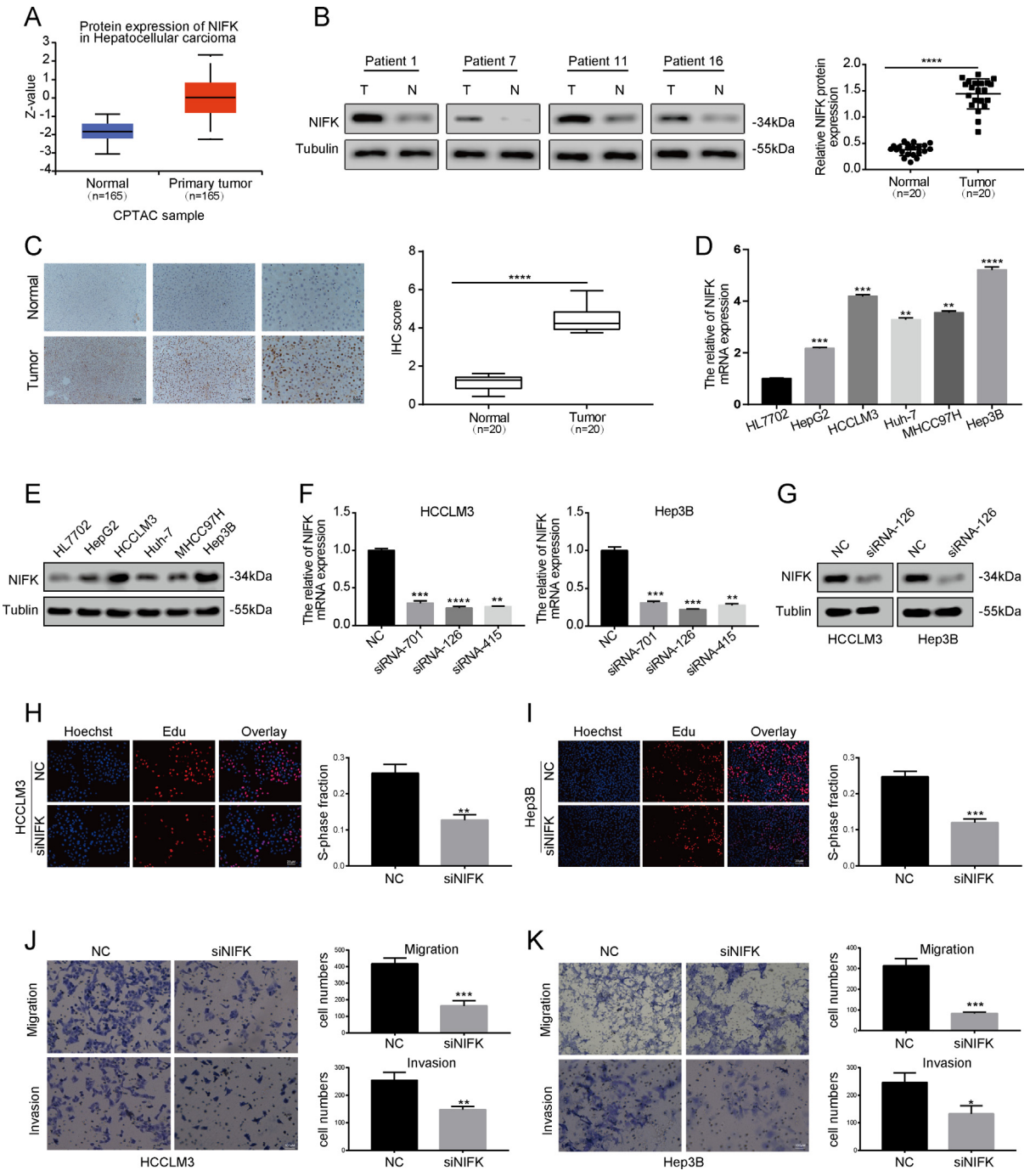

Fig. 6. Expression of NIFK in HCC tissues and knockdown of NIFK expression inhibits the proliferation, invasion and metastasis of HCC cells. (A) The protein expression of NIFK in HCC tissues and normal tissues in Ualcan database. (B) NIFK protein levels and quantitative analysis in human tissue specimens. (C) Representative images and quantification of NIFK staining in HCC tissues and normal liver tissues. (D) qPCR analysis comparing NIFK expression between normal and HCC cells; (E) Western blotting showed NIFK protein expression in normal liver cells and HCC cells; (F) and (G), qRT-PCR and western blot analyses were used to detect NIFK expression in HCCLM3 and Hep3B cells with siRNA knockdown; (H) and (I), EdU assay indicated a lower cell proliferation rate in the siNIFK group in HCCLM3 and Hep3B compared with the control; (J) and (K), Transwell assays showed that cell migration and invasion of HCCLM3 and Hep3B cells was significantly weaker in the siNIFK group than in the NC group $^{*}P < 0.05$; $^{**}P < 0.01$; $^{***}P < 0.001$; $^{****}P < 0.0001$.

Author contribution

- Study conception and design: W Shen; F Cheng.
- Data collection: LB Yuan; Z Wu.
- Analysis and interpretation of results: HZ Li; LB Yuan; Z Wu.
- Draft manuscript preparation: F Cheng; LB Yuan.
- Revision of the results and approval of the final version of the manuscript: W Shen.

Financial support

This work was supported by the National Natural Science Foundation of China (No.81860432) and the Natural Science Foundation of Jiangxi Provincial (No.20171BAB205064).

Conflict of interest

The authors declare no conflict of interest.

References

[1] Singal AG, Lampertico P, Nahon P. Epidemiology and surveillance for hepatocellular carcinoma: New trends. J Hepatol 2020;72(2):250–61. https://doi.org/10.1016/j.jhep.2019.08.025. PMid: 31954490.
[2] Sartoris R, Gregory J, Dioguardi Burgio M, et al. HCC advances in diagnosis and prognosis: Digital and Imaging. Liver Int 2021;41(Suppl 1):73–7. https://doi.org/10.1111/liv.14865. PMid: 34155790.
[3] Sung H, Ferlay J, Siegel RL, et al. Global cancer statistics 2020: GLOBOCAN estimates of incidence and mortality worldwide for 36 cancers in 185 countries. CA Cancer J Clin 2021;71(3):209–49. https://doi.org/10.3322/caac.21660. PMid: 33538338.
[4] Fitzmaurice C, Abate D, Abbasi N, et al. Global, regional, and national cancer incidence, mortality, years of life lost, years lived with disability, and disability-adjusted life-years for 29 cancer groups, 1990 to 2017: A systematic analysis for the global burden of disease study. JAMA Oncol 2019;5(12):1749–68. https://doi.org/10.1001/jamaoncol.2019.2996. PMid: 31560378.
[5] Kulik L, El-Serag HB. Epidemiology and management of hepatocellular carcinoma. Gastroenterology 2019;156(2):477–491.e1. https://doi.org/10.1053/j.gastro.2018.08.065. PMid: 30367835.
[6] Yang JD, Hainaut P, Gores GJ, et al. A global view of hepatocellular carcinoma: trends, risk, prevention and management. Nat Rev Gastroenterol Hepatol 2019;16(10):589–604. https://doi.org/10.1038/s41575-019-0186-y. PMid: 31439937.
[7] Yip TC, Lee HW, Chan WK, et al. Asian perspective on NAFLD-associated HCC. J Hepatol 2022;76(3):726–34. https://doi.org/10.1016/j.jhep.2021.09.024. PMid: 34619251.
[8] Malek NP, Schmidt S, Huber P, et al. The diagnosis and treatment of hepatocellular carcinoma. Dtsch Arztebl Int 2014;111(7):101–6. https://doi.org/10.3238/arztebl.2014.0101. PMid: 24622679.
[9] Takagi M, Sueishi M, Saiwaki T, et al. A novel nucleolar protein, NIFK, interacts with the forkhead associated domain of Ki-67 antigen in mitosis. J Biol Chem 2001;276(27):25386–91. https://doi.org/10.1074/jbc.M102227200. PMid: 11342549.
[10] Scholzen T, Gerdes J. The Ki-67 protein: from the known and the unknown. J Cell Physiol 2000;182(3):311–22. https://doi.org/10.1002/(SICI)1097-4652(200003)182:3<311::AID-JCP1>3.0.CO;2-9. PMid: 10653597.
[11] Menon SS, Guruvayoorappan C, Sakthivel KM, et al. Ki-67 protein as a tumour proliferation marker. Clin Chim Acta 2019;491:39–45. https://doi.org/10.1016/j.cca.2019.01.011. PMid: 30653951.
[12] Byeon IJ, Li H, Song H, et al. Sequential phosphorylation and multisite interactions characterize specific target recognition by the FHA domain of Ki67. Nat Struct Mol Biol 2005;12(11):987–93. https://doi.org/10.1038/nsmb1008. PMid: 16244663.
[13] Schlosser I, Hölzel M, Mürnseer M, et al. A role for c-Myc in the regulation of ribosomal RNA processing. Nucleic Acids Res 2003;31(21):6148–56. https://doi.org/10.1093/nar/gkg794. PMid: 14576301.
[14] Musgrove EA, Sergio CM, Loi S, et al. Identification of functional networks of estrogen- and c-Myc-responsive genes and their relationship to response to tamoxifen therapy in breast cancer. PLoS One 2008;3(8):e2987. https://doi.org/10.1371/journal.pone.0002987. PMid: 18714337.
[15] Abujarour R, Efe J, Ding S. Genome-wide gain-of-function screen identifies novel regulators of pluripotency. Stem Cells 2010;28(9):1487–97. https://doi.org/10.1002/stem.472. PMid: 20629179.
[16] Savkur RS, Olson MO. Preferential cleavage in pre-ribosomal RNA byprotein B23 endoribonuclease. Nucleic Acids Res 1998;26(19):4508–15. https://doi.org/10.1093/nar/26.19.4508. PMid: 9742256.
[17] Lin TC, Su CY, Wu PY, et al. The nucleolar protein NIFK promotes cancer progression via CK1α/β-catenin in metastasis and Ki-67-dependent cell proliferation. Elife 2016;5:e11288. https://doi.org/10.7554/eLife.11288. PMid: 26984280.
[18] Blum A, Wang P. Zenklusen JC. SnapShot: TCGA-Analyzed Tumors. Cell 2018;173(2):530. https://doi.org/10.1016/j.cell.2018.03.059. PMid: 29625059.
[19] Yu G, Wang LG, Han Y, et al. clusterProfiler: an R package for comparing biological themes among gene clusters. Omics 2012;16(5):284–7. https://doi.org/10.1089/omi.2011.0118. PMid: 22455463.
[20] Chandrashekar DS, Bashel B, Balasubramanya SAH, et al. UALCAN: A portal for facilitating tumor subgroup gene expression and survival analyses. Neoplasia 2017;19(8):649–58. https://doi.org/10.1016/j.neo.2017.05.002. PMid: 28732212.
[21] Chandrashekar DS, Karthikeyan SK, Korla PK, et al. UALCAN: An update to the integrated cancer data analysis platform. Neoplasia 2022;25:18–27. https://doi.org/10.1016/j.neo.2022.01.001. PMid: 35078134.
[22] Li T, Fan J, Wang B, et al. TIMER: A web server for comprehensive analysis of tumor-infiltrating immune cells. Cancer Res 2017;77(21):e108–10. https://doi.org/10.1158/0008-5472.CAN-17-0307. PMid: 29092952.
[23] Cheng F, Mohanmed MM, Li Z, et al. Capn4 promotes colorectal cancer cell proliferation by increasing MAPK7 through activation of the WNT/β-Catenin pathway. Exp Cell Res 2018;363(2):235–42. https://doi.org/10.1016/j.yexcr.2018.01.013. PMid: 29331389.
[24] Zeng F, Zhang Y, Han X, et al. Employing hypoxia characterization to predict tumour immune microenvironment, treatment sensitivity and prognosis in hepatocellular carcinoma. Comput Struct Biotechnol J 2021;19:2775–89. https://doi.org/10.1016/j.csbj.2021.03.033. PMid: 34093992.
[25] Mossanen JC, Tacke F. Role of lymphocytes in liver cancer. Oncoimmunology 2013;2(11):e26468. https://doi.org/10.4161/onci.26468. PMid: 24498546.
[26] Anwanwan D, Singh SK, Singh S, et al. Challenges in liver cancer and possible treatment approaches. Biochim Biophys Acta Rev Cancer 2020;1873(1):188314. https://doi.org/10.1016/j.bbcan.2019.188314. PMid: 31682895.
[27] Tabrizian P, Jibara G, Shrager B, et al. Recurrence of hepatocellular cancer after resection: patterns, treatments, and prognosis. Ann Surg 2015;261(5):947–55. https://doi.org/10.1097/SLA.0000000000000710. PMid: 25010665.
[28] Craig AJ, Villanueva A. Liver capsule: Molecular-based signatures in hepatocellular carcinoma. Hepatology 2016;63(6):2018. https://doi.org/10.1002/hep.28489. PMid: 26856972.
[29] Lyman SK, Gerace L, Baserga SJ. Human Nop5/Nop58 is a component common to the box C/D small nucleolar ribonucleoproteins. RNA 1999;5(12):1597–604. https://doi.org/10.1017/S1355838299991288. PMid: 10606270.
[30] Wang J, Huang R, Huang Y, et al. Overexpression of NOP58 as a prognostic marker in hepatocellular carcinoma: A TCGA data-based analysis. Adv Ther 2021;38(6):3342–61. https://doi.org/10.1007/s12325-021-01762-2. PMid: 34014550.
[31] He S, Tang S. WNT/β-catenin signaling in the development of liver cancers. Biomed Pharmacother 2020;132:110851. https://doi.org/10.1016/j.biopha.2020.110851. PMid: 33080466.
[32] Delire B, Stärkel P. The Ras/MAPK pathway and hepatocarcinoma: pathogenesis and therapeutic implications. Eur J Clin Invest 2015;45(6):609–23. https://doi.org/10.1111/eci.12441. PMid: 25832714.
[33] Chen J, Gingold JA, Su X. Immunomodulatory TGF-β signaling in hepatocellular carcinoma. Trends Mol Med 2019;25(11):1010–23. https://doi.org/10.1016/j.molmed.2019.06.007. PMid: 31353124.
[34] Zhu C, Ho YJ, Salomao MA, et al. Notch activity characterizes a common hepatocellular carcinoma subtype with unique molecular and clinicopathologic features. J Hepatol 2021;74(3):613–26. https://doi.org/10.1016/j.jhep.2020.09.032. PMid: 33038431.
[35] Oura K, Morishita A, Tani J, et al. Tumor immune microenvironment and immunosuppressive therapy in hepatocellular carcinoma: a review. Int J Mol Sci 2021;22(11). https://doi.org/10.3390/ijms22115801. PMid: 34071550.
[36] Heinrich B, Gertz EM, Schäffer AA, et al. The tumour microenvironment shapes innate lymphoid cells in patients with hepatocellular carcinoma. Gut 2022;71(6):1161–75. https://doi.org/10.1136/gutjnl-2021-325288. PMid: 34340996.